

Supplemental Information

Contact Resonance and Force Volume Working Principles

Contact resonance and force volume are two methods of measuring mechanical properties in the nanoscale with an AFM instrument. Each is suited to materials with different hardness ranges.

Contact resonance atomic force microscopy (CR) is a method of measuring viscoelastic properties (storage and loss modulus). By vibrating the sample at a selected frequency range and then measuring the resonant frequencies induced in the probe/sample system and comparing how these resonant frequencies shift compared to a known reference sample,

Two models are used in CR calculations; (i) Euler-Bernoulli beam theory to relate tip/sample resonant frequency to the stiffness of tip-sample, and (ii) a combination of Hertz and Derjaguin-Muller-Toporov (DMT) contact models to relate the tip-sample stiffness and the sample modulus [1,2]. Then, by using Hertzian contact mechanics for a spherical indenter and DMT model to include an adhesion force and using the material and geometric properties of the tip, the reduced modulus of the sample can be found, and then the storage and loss moduli [2–4].

Force volume (FV) is a second method for measuring mechanical properties with an AFM probe. It is conducted by recording the force-distance (f-z) curve of the AFM tip as it approaches the sample, interacts with the sample surface by Van der Waals forces, contacts the sample, and lifts off. The shape of this curve is analyzed to determine multiple properties, including modulus and adhesion. Multiple contact mechanics models can be used to model the probe and sample, similar to CR [5]. FV accuracy is dependent on matching the probe cantilever stiffness to the modulus range of the sample [6,7]. As composite electrode components can have a wide range of modulus values, it is challenging to fully characterize an electrode using FV with a single probe.

Scanning spreading resistance microscopy working principle [9,10]

Scanning spreading resistance microscopy (SSRM) is based on the contact mode of atomic force microscopy (AFM), where a bias voltage is applied between the probe and the sample and the current through the probe is measured. SSRM maps the local resistance beneath the probe in a hemispherical volume with a radius of approximately 50 nm. The AFM is set up in an argon-filled glovebox to prevent air exposure, and a logarithmic scale current amplifier with a wide

resistance range of 10^3 to $10^{14} \Omega$ is used for resistance measurement. A bias voltage is applied to the sample, while the probe is floating grounded. The measured resistance is the sum along the current path. The resistance at the back contact is much smaller than the measured resistance and not a contributing factor. To minimize the probe/sample contact resistance, the probe is pressed into the sample with a relatively large contact force of ~ 1 mN, ensuring that the measured resistance is predominantly due to the sample's spreading resistance. The spreading resistance is further dominated by the local resistance right beneath the probe as the current route increases rapidly with distancing away from the probe.

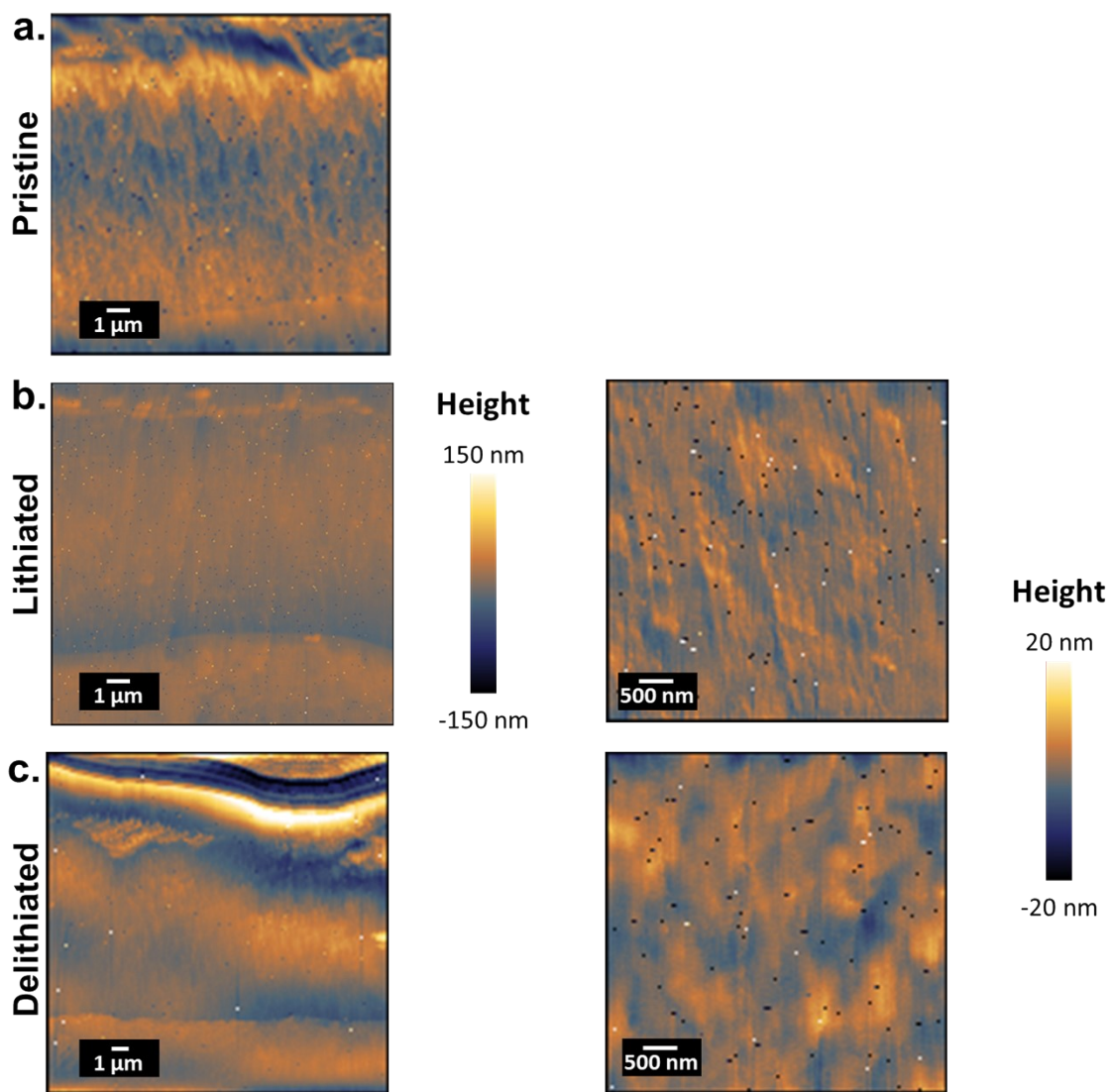


Figure S1: Height maps taken during CR-FV measurements corresponding to Figure 2 for the a) pristine, b) lithiated, and c) delithiated samples.

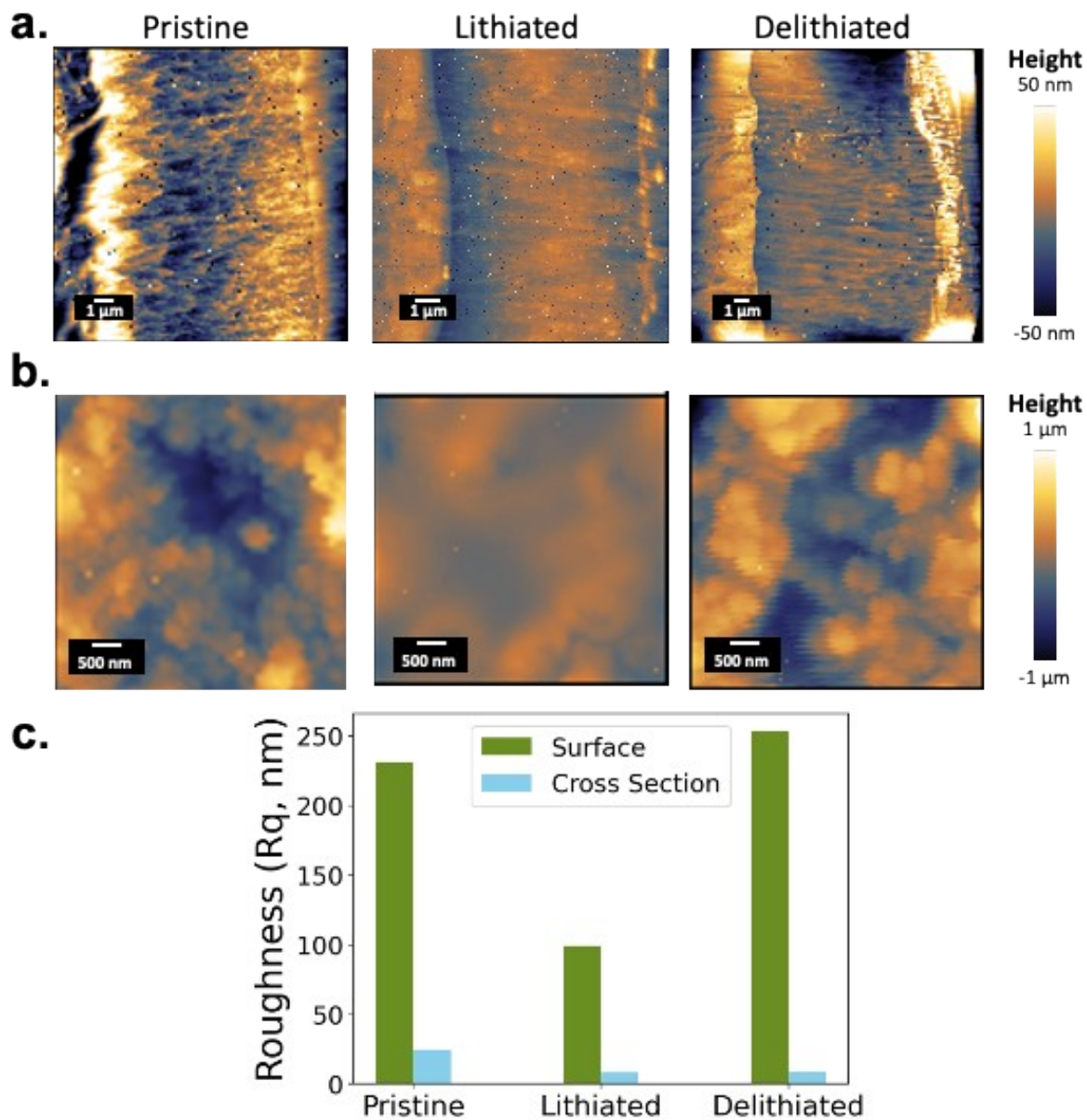


Figure S2: Height maps taken during CR-FV measurements for a) cross sectional maps, b) surface maps. c) Average roughness values from multiple sites on each sample showing decrease in roughness of polished cross sectional maps.

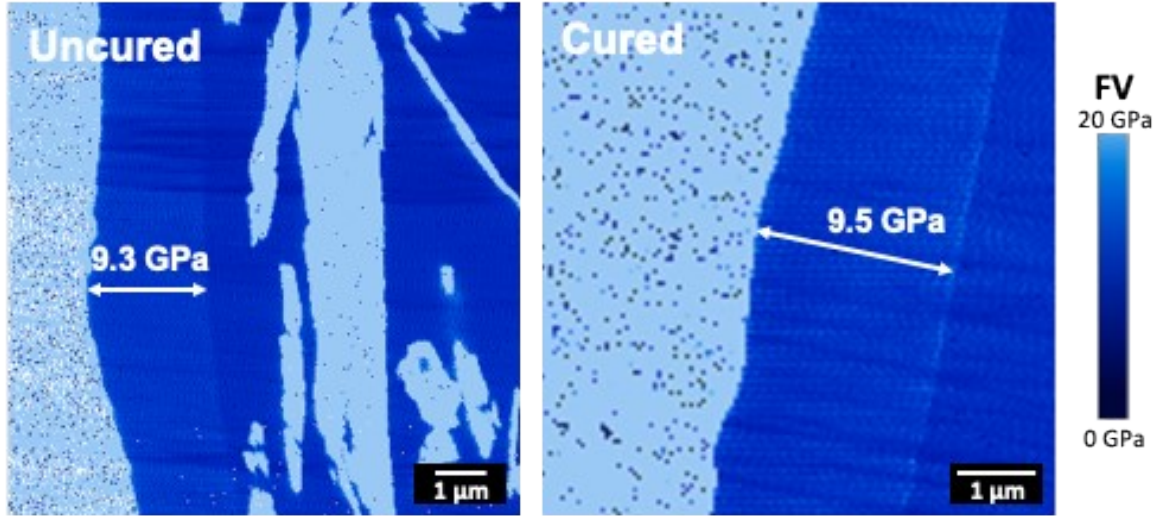
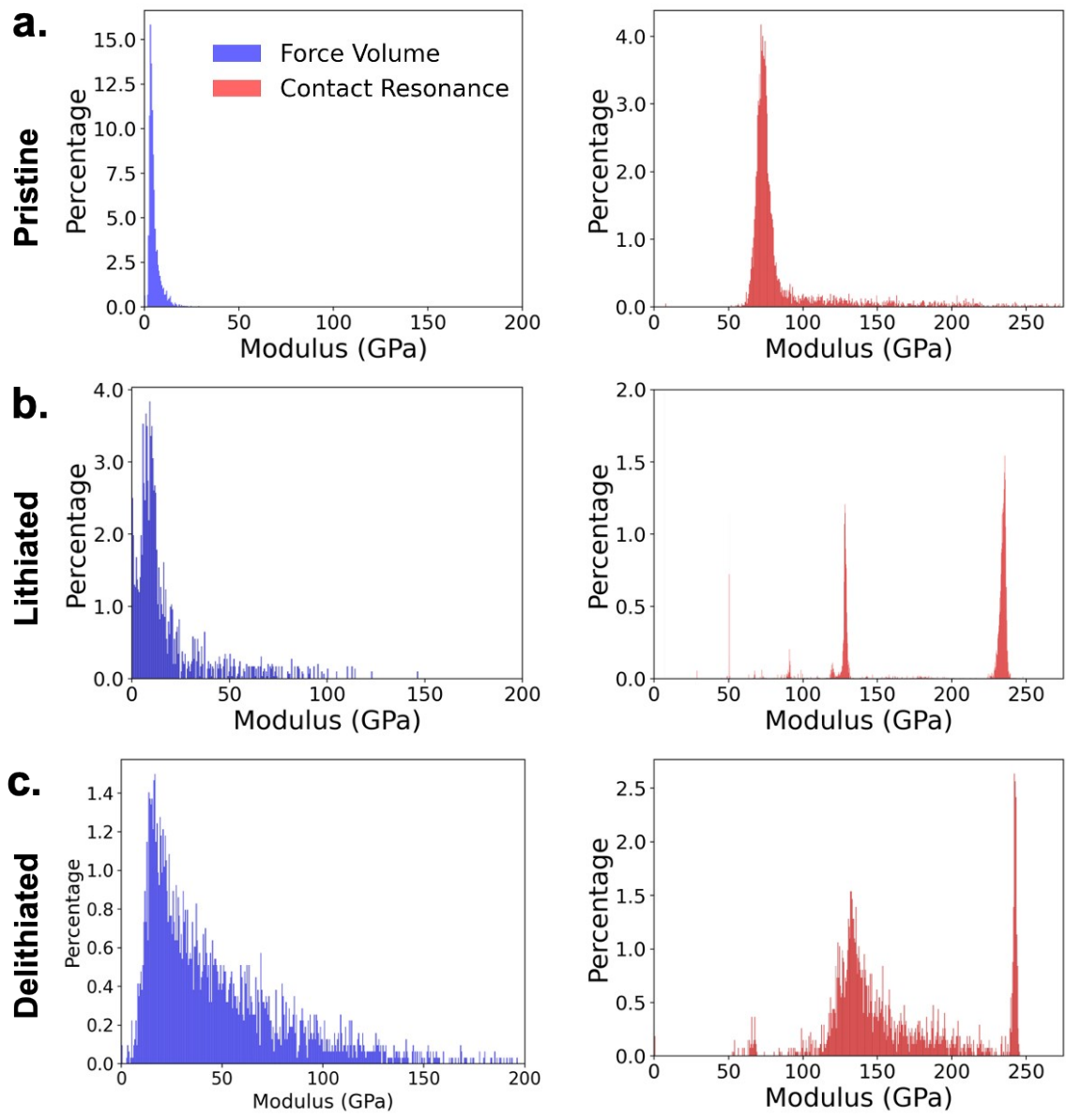


Figure S3: Cross sectional force volume modulus maps of cured and uncured binder-only samples with a similarly low modulus.



Figures S4: Additional histograms of CR-FV data of additional areas of the pristine, lithiated, and delithiated samples.

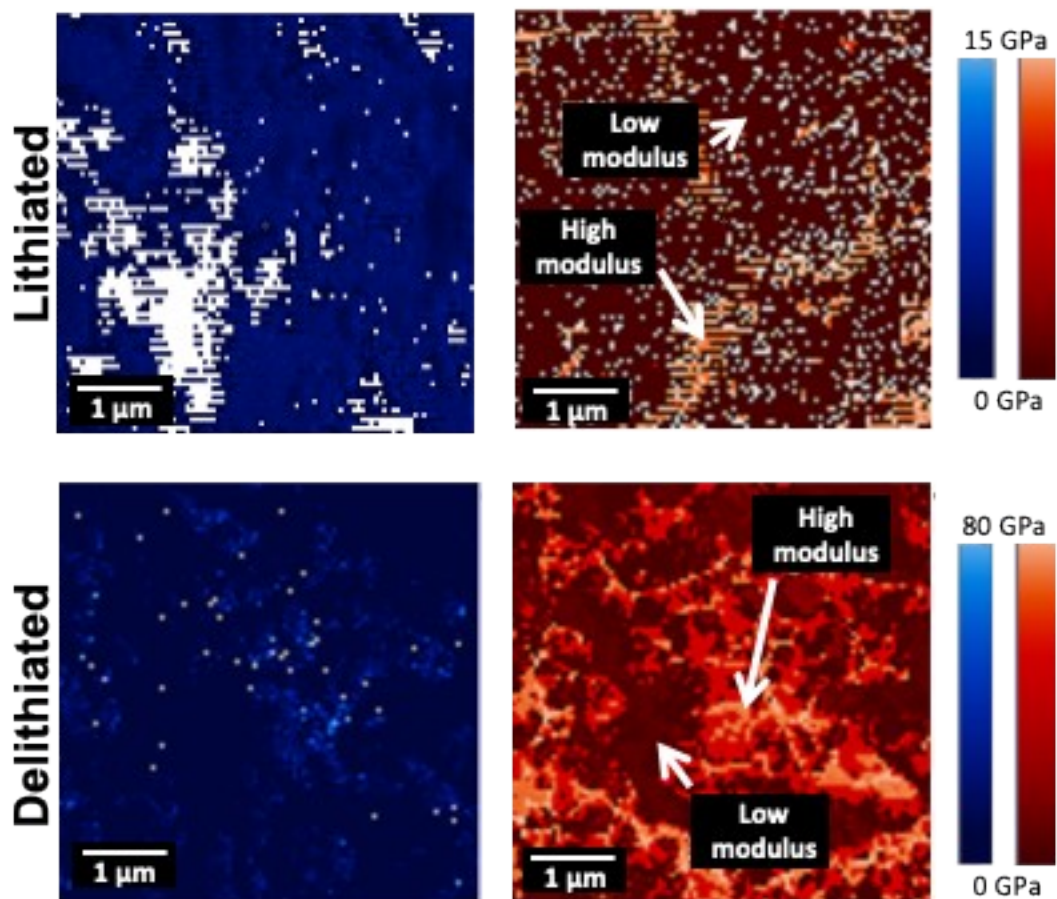


Figure S5: CR-FV maps taken on the surfaces of lithiated and delithiated electrode surfaces.

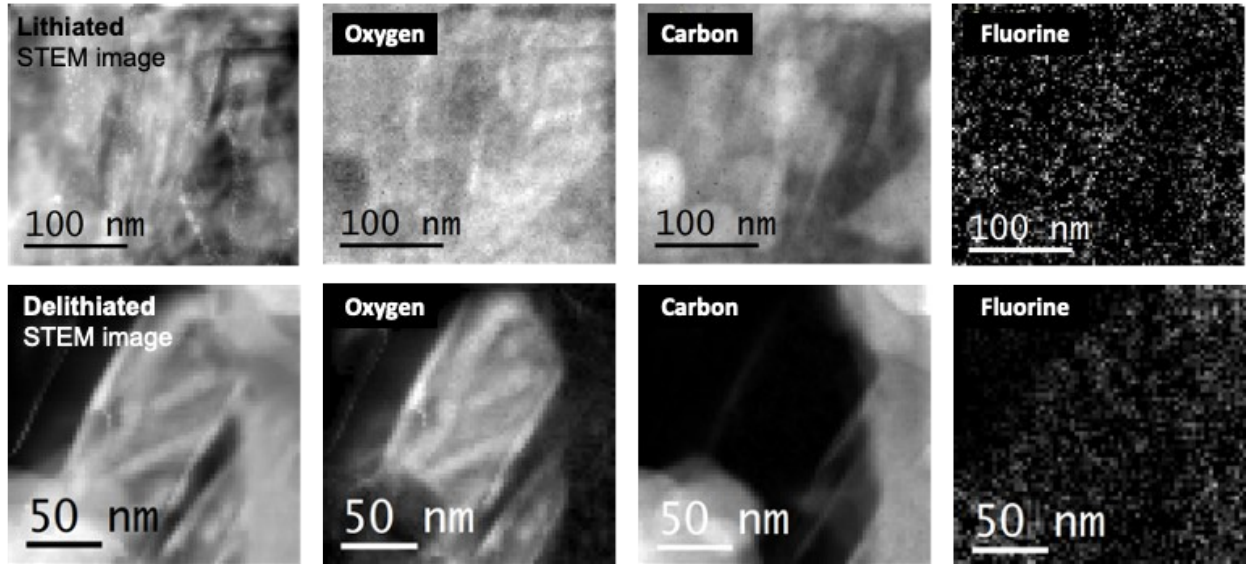


Figure S6: Additional STEM-EELS maps on the lithiated and delithiated samples showing oxygen, carbon, and fluorine.

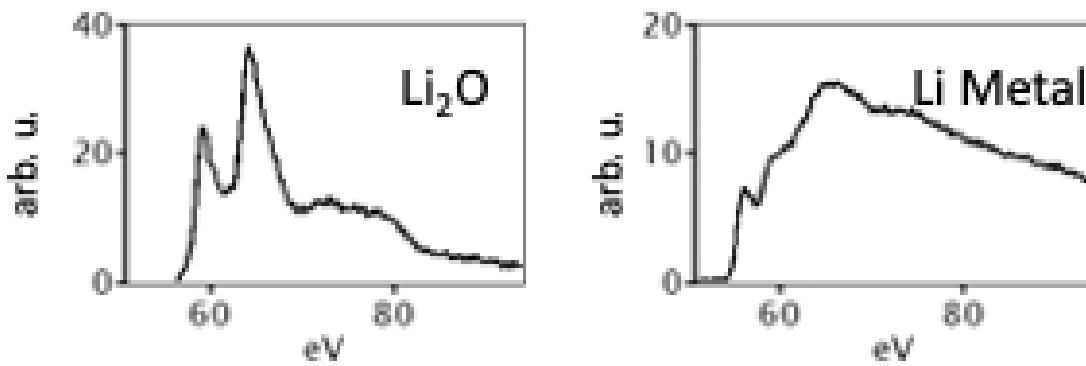


Figure S7: Electron energy loss spectra for Li_2O and Li metal obtained from reference samples.

These spectra are consistent with other reported spectra [8].

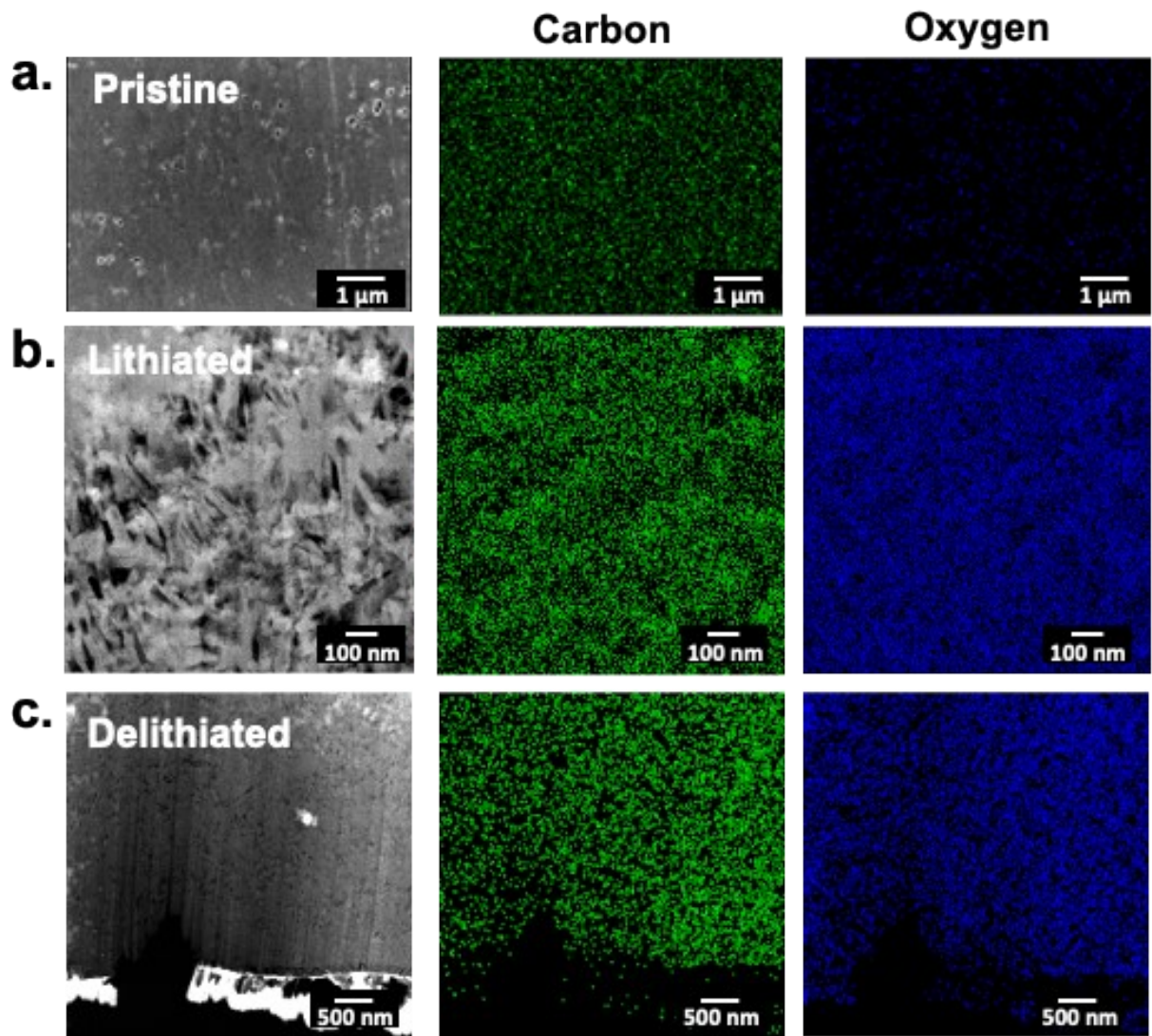


Figure S8: Cross sectional EDS maps of the a) pristine, b) lithiated, and c) delithiated samples showing uniform distribution of carbon and oxygen at a larger scale than the STEM-EELS maps.

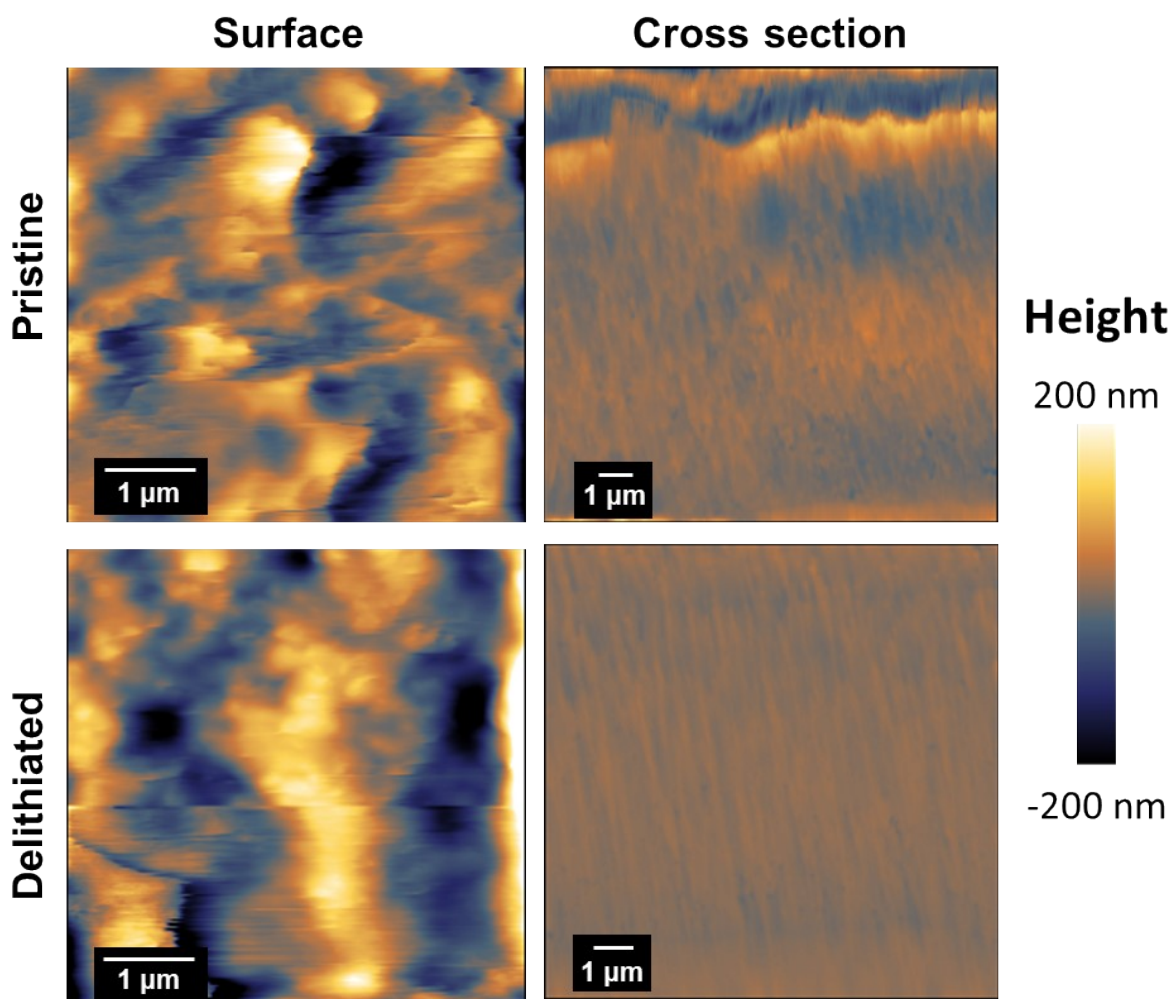


Figure S9: Height maps corresponding to Figure 5 for pristine and delithiated samples.

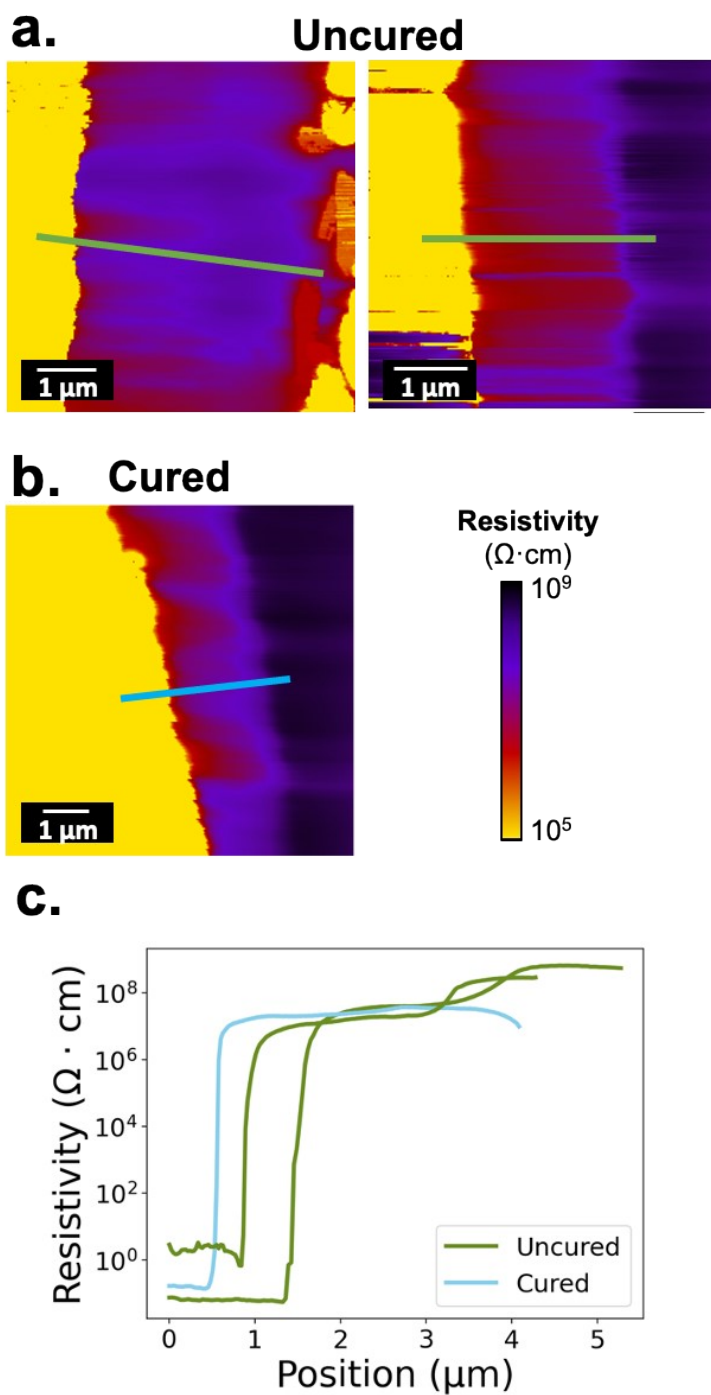


Figure S10: Cross sectional resistivity maps of a) uncured and b) cured PI-only samples with c) corresponding resistivity line plots. The PI is highly resistive and there is no significant change after curing.

Supplemental Information References

- [1] R. Wagner, R.J. Moon, A. Raman, Mechanical properties of cellulose nanomaterials studied by contact resonance atomic force microscopy, *Cellulose* 23 (2016) 1031–1041. <https://doi.org/10.1007/s10570-016-0883-4>.
- [2] B.V. Derjaguin, V.M. Muller, Y.P. Toporov, Effect of contact deformations on the adhesion of particles, *J. Colloid Interface Sci.* 53 (1975) 314–326. [https://doi.org/10.1016/0021-9797\(75\)90018-1](https://doi.org/10.1016/0021-9797(75)90018-1).
- [3] J.P. Killgore, D.G. Yablou, A.H. Tsou, A. Gannepalli, P.A. Yuya, J.A. Turner, R. Proksch, D.C. Hurley, Viscoelastic property mapping with contact resonance force microscopy, *Langmuir* 27 (2011) 13983–7. <https://doi.org/10.1021/la203434w>.
- [4] X. Zhou, J. Fu, F. Li, Contact resonance force microscopy for nanomechanical characterization: Accuracy and sensitivity, *J. Appl. Phys.* 114 (2013).
- [5] B. Cappella, G. Dietler, Force-distance curves by atomic force microscopy, *Surf. Sci. Rep.* 34 (1999) 1–104. [https://doi.org/10.1016/S0167-5729\(99\)00003-5](https://doi.org/10.1016/S0167-5729(99)00003-5).
- [6] Force-Distance Measurements, Bruker.
- [7] Dimension Icon User Guide, Bruker (2011).
- [8] V. Mauchamp, F. Boucher, G. Ouvrard, P. Moreau, Ab initio simulation of the electron energy-loss near-edge structures at the LiK edge in Li, Li₂O, and LiMn₂O₄, *Physical Review B* 74 (2006). <https://doi.org/10.1103/PhysRevB.74.115106>.
- [9] P. Eyben, M. Xu, N. Duhayon, T. Clarysse, S. Callewaert, W. Vandervorst, Scanning spreading resistance microscopy and spectroscopy for routine and quantitative two-dimensional carrier profiling, *Journal of Vacuum Science & Technology B: Microelectronics and Nanometer Structures Processing, Measurement, and Phenomena* 20 (2002) 471–478. <https://doi.org/10.1116/1.1424280>.
- [10] P. Eyben, F. Clemente, K. Vanstreels, G. Pourtois, T. Clarysse, E. Duriau, T. Hantschel, K. Sankaran, J. Mody, W. Vandervorst, K. Mylvaganam, L. Zhang, Analysis and modeling of the high vacuum scanning spreading resistance microscopy nanocontact on silicon, *Journal of Vacuum Science & Technology B, Nanotechnology and Microelectronics: Materials, Processing, Measurement, and Phenomena* 28 (2010) 401–406